Journal Pre-proof

Genetic and functional analyses of Cutibacterium acnes isolates reveal association of a linear plasmid with skin inflammation.

Alan M. O'Neill, Kellen J. Cavagnero, Jason S. Seidman, Livia Zaramela, Yang Chen, Fengwu Li, Teruaki Nakatsuji, Joyce Y. Cheng, Yun L. Tong, Tran H. Do, Samantha L. Brinton, Tissa R. Hata, Robert L. Modlin, Richard L. Gallo

PII: S0022-202X(23)02415-6

DOI: https://doi.org/10.1016/j.jid.2023.05.029

Reference: JID 3922

To appear in: *The Journal of Investigative Dermatology*

Received Date: 14 January 2023

Revised Date: 19 April 2023

Accepted Date: 4 May 2023

Please cite this article as: O'Neill AM, Cavagnero KJ, Seidman JS, Zaramela L, Chen Y, Li F, Nakatsuji T, Cheng JY, Tong YL, Do TH, Brinton SL, Hata TR, Modlin RL, Gallo RL, Genetic and functional analyses of Cutibacterium acnes isolates reveal association of a linear plasmid with skin inflammation., *The Journal of Investigative Dermatology* (2023), doi: https://doi.org/10.1016/j.jid.2023.05.029.

Title: Genetic and functional analyses of Cutibacterium acnes isolates reveal association of a linear plasmid with skin inflammation.

Authors: Alan M. O'Neill[1], Kellen J. Cavagnero[1], Jason S. Seidman[2], Livia Zaramela[3], Yang Chen[1,3], Fengwu Li[1], Teruaki Nakatsuji[1], Joyce Y. Cheng[1], Yun L. Tong[1], Tran H. Do[4], Samantha L. Brinton[1], Tissa R. Hata[1], Robert L. Modlin[4], Richard L. Gallo[1]*

Affiliations:

[1]Department of Dermatology, University of California, San Diego; La Jolla, CA 92093 USA

[2]Department of Cellular and Molecular Medicine, University of California, San Diego; La Jolla, CA 92093, USA.

[3]Department of Pediatrics, University of California, San Diego, 9500 Gilman Drive, La Jolla, CA 92093-0760, USA.

[4]Division of Dermatology, University of California Los Angeles; Los Angeles, CA, 90095, USA.

* Corresponding author: Richard L. Gallo, Department of Dermatology, Alman Clinical and Translational Research Institute, 9452 Medical Center Drive, University of California San Diego, La Jolla, CA, 92093. Tel: +1 858-882-4608. Email: rgallo@health.ucsd.edu.

ORCiDs:

Alan M. O'Neill: 0000-0002-5892-6477

Kellen J. Cavagnero: 0000-0003-4160-6394

Jason S. Seidman: 0000-0001-7626-5759

Livia Zaramela: 0000-0002-1065-3799

Yang Chen: 0000-0002-0164-8971

Fengwu Li: 0000-0001-5092-770X

Teruaki Nakatsuji: 0000-0002-6187-2991

Joyce Y. Cheng: 0000-0002-7317-7486

Yun L. Tong: 0000-0003-2003-1843

Tran H. Do: 0000-0001-6317-9202

Samantha L. Brinton: 0000-0003-1014-2566

Tissa R. Hata: 0000-0003-0183-4210

Robert L. Modlin: 0000-0003-4720-031X

Richard L. Gallo: 0000-0002-1401-7861

This work was presented at the 69th annual Montagna Symposium on the Biology of Skin, "Microbes, Autoimmunity & Cancer," held October 20 - 24, 2022.

Abstract:

Cutibacterium acnes (*C. acnes*) is a commensal bacterium on skin that is generally well tolerated but different strain-types have been hypothesized to contribute to the disease acne vulgaris. To understand how some strain-types might contribute to skin inflammation we generated a repository of *C. acnes* isolates from skin swabs of healthy and acne subjects and assessed their strain-level identity and capacity to stimulate cytokine release. Phylotype II K-type strains were more frequent on healthy and non-lesional skin of acne subjects compared to those isolated from lesions. Phylotype IA-1 C-type strains were increased on lesional skin compared to healthy skin. The capacity to induce cytokines from cultured monocyte-derived dendritic cells was opposite to this action on sebocytes and keratinocytes and did not correlate with the strain-types associated with disease. Whole genome sequencing revealed a linear plasmid in high-inflammatory isolates within similar strain-types that had different proinflammatory responses. Single-cell RNA sequencing of mouse skin following intradermal injection showed strains containing this plasmid induced a higher inflammatory response in dermal fibroblasts. These findings revealed that *C. acnes* strain-type is insufficient to predict inflammation and that carriage of a plasmid could contribute to disease.

Main text:

INTRODUCTION

Acne vulgaris is a disease of the pilosebaceous unit and the eighth most prevalent disease worldwide, affecting 9.4% of the global population (Hay et al. 2014; Vos et al. 2012). The high disease prevalence and its associated clinical, psychosocial, and economic impact lead to a

significant disease burden. *C. acnes* is a gram-positive, facultative anaerobic bacterium that is the most abundant bacterial member of the skin microbiome, colonizing lipid-rich areas of the skin at densities of up to 10^6 colony-forming units/cm^2 (Leyden et al. 1998). Despite its abundance on normal skin, *C. acnes* is considered a major contributor to the development of acne and the host inflammatory response. Furthermore, despite the presence of *C. acnes* in all skin follicles, only a small proportion of follicles exhibit the inflammation characteristic of acne, even in severe cases (Ramli et al. 2012). Thus, the bacterial-host pathogenic determinants that regulate these irregular inflammatory events in acne remain incompletely understood.

The precise role of *C. acnes* in the etiology of acne vulgaris has remained elusive for decades due to similar bacterial CFU counts in follicles from acne and healthy patients (Puhvel et al. 1975). More recent analysis of the acne skin microbiome confirmed similar relative abundances of *C. acnes* in the follicles isolated from acne and healthy skin (Fitz-Gibbon et al. 2013). However, more detailed analyses revealed differences in the *C. acnes* strain populations between patients with acne and those without acne. *C. acnes* strains found on acne skin most often belong to phylotype IA-1 (representing ribotypes RT4, RT5, and RT8), whereas health-associated strains belong to other phylotypes of IA-2, IB, or II (representing RT1, RT2, RT3 and RT6) (Barnard et al. 2016; Fitz-Gibbon et al. 2013). Since then, other studies have adopted high resolution sequencing approaches to type *C. acnes* strains and have generally confirmed the finding that phylotype IA-1 is more abundant on subjects with acne (Conwill et al. 2022; Hall et al. 2018). Furthermore, some strains showed higher potential to induce cytokines from cultured monocytes (Yu et al. 2016). These observations have led to the hypothesis that *C. acnes* phylotypes have a role in disease development.

In this study, we sought to better understand the factors that predict *C. acnes* inflammatory potential. To do this, we collected clinical *C. acnes* isolates from lesional and non-lesional skin of acne patients as well as from the skin of healthy volunteers and screened this repository for the capacity to induce cytokines and induce inflammation when injected into mice. We report that *C. acnes* strain types associated with acne are found on acne lesional skin, but not non-lesional skin, and that inflammatory potential is not exclusively associated with specific strain-types. By combining whole genome sequencing with functional assessment of *C. acnes* isolates we observed that the presence of a linear plasmid was a predictor of inflammatory potential. These observations provide greater understanding of how *C. acnes* contributes to inflammation in acne.

RESULTS

Epithelial inflammatory responses to health- and disease-associated *C. acnes* strains are cell-type dependent.

To investigate the host response to *C. acnes* we compared the response of different host cells to six health- and acne- associated strains. *C. acnes* isolates were cultured in nutrient and lipid-rich, anoxic conditions for 5 days, then sterile filtered and this conditioned media was added onto culture of host cells for 24 h. In agreement with published literature (Nagy et al. 2005; Yu et al. 2016), acne-derived strains (C-type strains HL096PA1, HL043PA1 and HL005PA1) induced greater levels of IL-10 and IFNγ from human monocyte-derived dendritic cells (hDC) than health-associated K-type strains HL110PA3, HL110PA4 and HL042PA3 (**Fig.1A**). However, the opposite relationship was observed upon exposure of normal human keratinocytes (NHEK).

These host cells had less IL-8 and IL-6 release after exposure to acne-associated C-type strains compared to the health-associated K-type strains (**Fig.1B**). In addition, cytokine levels from NHEKs or hDCs were similar upon treatment with conditioned supernatant of all three strains belonging to phylotypes IA-1 or II, suggesting a high degree of similarity amongst the strains. As *C. acne*s primarily interacts with epithelial cells on the skin surface or sebocyte cells in sebaceous glands (Sanford et al. 2019; Sanford et al. 2016), further analysis focused on these cell types.

C. acnes sequence type is associated with acne lesions but does not predict capacity to induce cytokine release by sebocytes.

We next generated a larger repository of *C. acnes* isolates (>1000) collected from swabs of facial skin sites of acne patients as well as facial skin of healthy volunteers (**Fig. 2A**). Surface swabbing is a convenient method to sample the acne microbiome and provides similar diversity profiles to extracted follicular casts (Hall et al. 2018). Swabs were collected from both lesional and adjacent non-lesional sites of twelve subjects with acne to explore the local diversity of *C. acnes* and compare to healthy skin sites of eight subjects without acne. Next, 219 *C. acnes* isolates were selected based on optical density readings (OD600) >1.0 and strain-typed using single-locus sequence type (SLST). A high frequency of phylotype IA-1 C-type was observed on acne lesional skin, whilst only a few were detected on non-lesional skin, and none recovered from healthy skin (**Fig.2B**). In contrast, phylotype II K-type strains were strongly associated with healthy and non-lesional skin, but rarely detected on lesional skin sites. Although prior reports suggested that specific clonal complexes (CC) of phylotype IA-1 (namely CC1, CC3 and CC4) were predominantly associated with acne (McDowell et al. 2012), our observations expand upon

this finding to show that phylotype IA1 CC3 types (C1/C2 by SLST) are dominant on acne lesional sites and rarely detected on non-lesional skin of acne subjects.

Next, the inflammatory capacity of individual *C. acnes* isolates was measured by assessment of IL-8 secretion. The sebocyte cell line (SEB-1) was selected for screening as these cells respond similarly to NHEKs (Sanford et al. 2019)10) but show less batch-to-batch variability than primary cell cultures and are thus more suitable for high throughput screening. No significant difference in IL-8 release was observed based on the site of recovery, disease association, or comparing C-types to K-types (**Fig. 2C-E**). However, further resolution of additional sequence types (A, C, D, E, F, H, K) showed significant differences in IL-8 release between strains isolated within both healthy subjects and lesions from acne subjects (**Fig. 2F,G**). Furthermore, substantial variation in IL-8 release was observed for isolates within the same sequence type. This suggested that important functional differences exist within similar sequence types. To assess these at greater depth, twelve isolates belonging to K1, K2, C1, C2 and H1 types were selected, validated and named according to their sequence type and capacity to induce low, medium (med) or high cytokine responses in SEB-1 cells (**Fig. 2H**). Variation in potential growth density was observed within this group but this did not correlate with differences in the capacity to promote IL-8 release (**Fig. 2H**)

A linear plasmid in *C. acnes* is associated with an increased capacity to induce IL8.

The panel of 12 strains were next subjected to whole genome sequencing to search for the presence of genetic elements associated with inflammation. Analysis of the core genome of the identical sequence types revealed an expected high degree of gene conservation between strains.

However, several strains contained distinct contigs with a GC content of (62-63%), which is approximately 2-3% higher than the chromosomal genome, suggesting the presence of a plasmid with similarity to a 56 kb linear plasmid belonging to type IA strain called pIMPLE-HL096PA1 (**Fig. 3A**) (Davidsson et al. 2017). We identified the presence of this plasmid in sequence contigs from high inflammatory strains, (35K2 high, 46C1 high, 61C2 high, and 44H1 high), and found protein-encoded genes in these plasmids with high sequence similarity to the annotated pIMPLE plasmid (**Suppl. Fig.1**). In contrast, none of the low or med inflammatory strains in the K-, C- or H-type strains contained the plasmid. To better assess a potential link for the presence of the plasmid with the release of IL-8, we PCR screened and identified additional plasmid-positive and plasmid-negative strains based on the presence or absence of the plasmid-encoded tight adhesion (tadA) gene (Davidsson et al. 2017). Overall, we detected a significant increase in IL-8 from several, but not all, plasmid-positive strains compared to strains that lacked a plasmid (**Fig. 3B**).

Having defined *C. acnes* strains with high and low inflammatory potential we next sought to better understand the global transcriptional response of the host to these strains. NHEKs were treated for 4 h with control bacterial culture media that was not conditioned by *C. acnes* (untreated), or with sterile conditioned medium from different strains of *C. acnes* (44H1 + Plasmid (high), 17H1 - plasmid (low), 46C1 + plasmid (high) and 42C1 – plasmid (low)). NHEK transcriptomes were analyzed by bulk RNA Seq. Gene ontology (GO)-based overrepresentation analysis of NHEKs treated with both H1 types revealed significant enrichment of genes relating to TNF, interleukin 10 and JAK-STAT signaling pathways for the plasmid-containing strain only (**Fig. 3C**). Likewise, in NHEKs treated with C1 type strains, the presence of the plasmid was associated with greater enrichment of genes associated with chemokine-mediated signaling and

cellular response to DNA damage stimulus (**Fig. 3D**). Examination of the expression of selected genes in the cytokine-mediated signaling GO term across all treatments revealed greater expression of chemokines CXCL1, CXCL2, CXCL3, and CXCL8 for the H1 and C1 plasmid-containing strains compared to their plasmid-absent counterparts (**Fig. 3E**). These observations supported prior ELISA-based screening that suggested strains containing the linear plasmid had greater pro-inflammatory potential.

Plasmid-positive strains promote greater tissue inflammation in mouse skin.

Since the capacity of *C. acnes* to promote greater inflammation in keratinocytes and sebocytes was associated with the presence of the plasmid, we examined if the plasmid also drives greater tissue inflammation. SKH1 mice were intradermally injected with four strains of *C. acnes* representing H1 and K2 sequence types with (+P) or without the plasmid (-P). 72 h post-infection, biopsies of the infected skin lesions were collected, and cytokine levels were quantified by ELISA. The total number of *C. acnes* by colony forming units (CFU) was also measured. Both the 44H1 and 35K2 plasmid-containing strains promoted greater tissue inflammation compared to their identical non-plasmid containing sequence types. Both IL-6 and CCL2 were significantly increased for the 44H1 +P strain compared to 17H1 -P strain and IL-1beta significantly enhanced for the K2 +P strain compared to K2 -P. (**Fig. 3F**). The recorded increase in inflammation by H1 and K2 +P strains was unlikely to be due to differences in bacterial survival or proliferation in the tissue since total CFU was not significantly different (**Fig. 3G**). This suggested a differential host immune response towards bacteria during dermal infection and validated previous data of inflammatory reactions to +P strains by NHEK and SEB-1 cells.

scRNA-Seq of *C. acnes*-infected mice reveals unique inflammatory fibroblast subsets associated with the linear plasmid.

Single cell RNA sequencing (scRNA-Seq) of *C. acnes*-infected mouse skin was next performed to identify the specific cell types that mediate the differential skin immune response to the plasmid-positive strains of *C. acnes*. SKH1 mice were injected with two C-type +P and -P *C. acnes* strains and the transcriptome for each major cell type was measured. Nine major cell types were identified and visualized using uniform manifold proximation and projection (UMAP) (**Fig. 4A**). The *C. acnes* plasmid-containing strain (+P) showed greater changes to the transcriptome compared to the plasmid-negative strains (-P), as demonstrated by the greater number of differentially expressed genes across all nine major cell types (**Fig. 4B**). Fibroblasts were the major cell types that responded to *C. acnes* infections, followed by keratinocytes and myeloid cells. GO term analysis revealed that the *C. acnes* +P strain promoted greater immune responses in fibroblasts (**Fig. 4C-D**), keratinocytes (**Fig. 4E-F**) and myeloid cells (**Fig. 4G-H**) compared to the -P strain, including GO networks relating to cytokine mediated signaling, and pathways associated with interleukin-1, interferon gamma and interferon beta responses, and IL-17 signaling. In Fibroblasts, major differentially expressed immune-related genes included *Cxcl10*, *Ccl7* and *C3* **(Fig. 4D**), which participate in anti-infectious immunity by immune cell recruitment during infection (Caetano et al. 2023). In addition, expression of the antimicrobial peptide-encoding gene Lipocalin 2 (*Lcn2*) was higher in +P activated fibroblasts and was previously found to be induced in lesional skin of acne patients and in response to intradermal injection of *C. acnes* in mice (Kelhälä et al. 2014; O'Neill et al. 2022). Overall, single cell

analysis of whole mouse tissue revealed greater inflammatory and host defense activation across several major cell types in response to *C. acnes* that harbor a linear plasmid.

DISCUSSION

In this study, we demonstrate that *C. acnes* isolates representing the same sequence type exhibit distinct inflammatory responses in host cells. Our findings show that *C. acnes* sequence types previously thought to be associated with the individual affected with acne do not reflect the disease susceptibility of the individual, but rather with the presence or absence of a lesion at the collection site. Furthermore, whole genome sequencing of a panel of high and low-inflammatory strains recovered from both acne lesions and normal skin revealed a linear plasmid associated with greater inflammation *in vitro* and *in vivo*. Transcriptional analysis of human cells and mouse tissue exposed to *C. acnes* strains containing this plasmid revealed induction of important inflammatory pathways relating to cytokine and chemokine-mediated signaling and responses to IL-1. These data indicate that subtle differences in the genetic and metabolic diversity of identical sequence types of *C. acnes* can induce markedly different inflammatory outcomes, suggesting some redundancy defining strain functionality exclusively on disease-association or sequence type alone.

C. acnes contains a linear plasmid initially identified by Kasimatis *et al*. (Kasimatis et al. 2013). It is described as a low copy, linear plasmid of 56 kb in size and contains a gene locus for tight adherence (tad) that codes for the biosynthesis of adhesive Flp (fimbrial low-molecular weight protein) pili, predicted to be involved in attachment. A previous study identified several plasmid-positive strains amongst different SLSTs indicating that plasmid carriage is not strictly

associated with a single phylotype or disease type (Davidsson et al. 2017). However, no study has yet demonstrated whether the plasmid is associated with inflammation. The linear plasmid has been shown to be functionally active with several plasmid-encoded proteins detected in secreted protein fractions of *C. acnes* (Holland et al. 2010). However, many plasmid-encoded genes have an unknown function and have yet to be characterized. Many plasmid-encoded proteins (provided in Suppl. Fig.1) showed a similar sequence similarity between 46.C1, 61.C2 and 44H1 strains but not for the 35K2 strain. Attempts to cure the plasmid from *C. acnes* strains using treatment with acridine orange and shifts to elevated temperature were attempted here, but ultimately unsuccessful. Other groups have reported the unstable nature of the plasmid in *C. acnes* (Scholz et al. 2016) and similarly, attempts to purify and concentrate the linear plasmid were also unsuccessful, potentially due to its reported low copy number (2-3 copies per cell) (Kasimatis et al. 2013).

Alternatively, intradermal injection of *C. acnes* into mouse skin revealed significantly greater inflammation for the plasmid-containing strain, with greater production of CCL2, IL-6 and IL-1beta compared to the non-plasmid-containing strain. scRNA-Seq revealed that the major cell type contributing to immune activation in response to the *C. acnes* plasmid were dermal fibroblasts. Keratinocytes also demonstrated a greater number of differentially expressed genes in response to the *C. acnes* plasmid as well as Myeloid cells, but to a much lesser extent. That fibroblasts showed greater immune activation than other skin cell types during infection with the *C. acnes* +P strain was not entirely unsuspected given the intradermal injection site and transient 3-day post analyses in this mouse model. A topical colonization model could be adopted to better determine keratinocyte responses more accurately to *C. acnes*, but to our knowledge has

not been described in the literature. Nevertheless, recent work has shown that *C. acnes* activates an adipogenic and host defense program in fibroblasts during acne development which is a major contributor to the pathophysiology of this disease (O'Neill et al. 2022).

In summary, these results provide greater insight into the genetic variables present in *C. acnes* that can trigger skin inflammation. Our findings demonstrate that individual colonization by a *C. acnes* sequence type does not predict susceptibility to disease. Although several factors produced by *C. acnes* can influence inflammatory potential, this study identifies an additional variable that can contribute to this complex disease. Further bacterial transcriptomic and proteomic analysis, as well as technological advances to improve the capacity to perform genetic modifications in *C. acnes* is required to identify the mechanism by which a plasmid may promote inflammatory potential. Acne is a disease of the holobiome (Bordenstein and Theis 2015), dependent of variables present in both the host and microbiome, and future progress requires coordinated study of both microbe and human cells.

MATERIALS AND METHODS

Human subjects and skin swab collection

All experiments involving human subjects were carried out according to protocols approved by the University of California, San Diego institutional review board (Project#140144). Written informed consent was obtained from all subjects. *C. acnes* clinical isolates were obtained by swabbing lesional and non-lesional facial skin sites of twelve patients with mild-moderate acne, as well as facial skin from eight healthy volunteers. Patients had no history of antibiotic use within 2 weeks prior to sampling. Non-lesional skin refers to non-inflamed skin sites that were

directly adjacent to the lesional inflamed skin site. Subjects included both males and females aged 18–24 years, with acne patients diagnosed with mild-to-moderate facial acne. Patients with acne at the time of sample collection were instructed to avoid any washing and cosmetic application to the skin sites in the preceding 24 hours. Healthy subjects also had no history of antibiotic use within 2 weeks prior to sampling nor had any history of inflammatory acne. For *C. acnes* strain collection, Puritan foam tipped swabs were first soaked in sterile saline solution and applied directly to the lesional, non-lesional and healthy skin sites. The swabs were then transferred to eppendorf tubes containing 20% glycerol in reinforced clostridial media (RCM). The swabs were incubated for 5 mins in each tube at room temperature with intermittent vortexing. Swabs were then transferred to -80°C until plating. Upon thawing, the tubes were vortexed once more and 100 µl removed and serially diluted onto brucella blood agar plates supplemented with Vitamin K, hemin, and 5% sheep's blood and incubated for 5 days at 37 °C in an AnaeroPak (Thermo Fisher Scientific, Waltham, MA).

Bacterial Strains and Bacterial Culture

C. acnes strains were grown on Brucella blood agar plates and grown for 5 days at 37° under anaerobic conditions. Single colony isolates were resuspended in 5 mL reinforced clostridial media (RCM) (BD Difco) and grown for 5-7 days at 37° under anaerobic conditions. For cellular bacterial supernatant treatment, bacteria were cultured in EpiLife cell culture medium (ThermoFisher) supplemented with RCM and 1% glycerol as a lipid source for 5 days (Sanford et al. 2019). Since undiluted RCM can exhibit some inflammatory activity, the bacterial conditioned supernatant was sterile filtered and inoculated onto cells at a final concentration of 15-20%, where indicated. For *in vivo* and antimicrobial experiments, bacteria were pelleted and

resuspended and diluted in fresh RCM to approximately 1 x 10^7 CFU. To examine the effects of *C. acnes in vitro*, supernatants were filtered through a 0.22 μm filter. Sterile filtrate was then added to cultured cells. Of the sequenced *C. acnes* strains, the following were isolated from healthy skin (21.K2low, 35.K2high, 48.K1med), acne non-lesional skin (2.K1low, 21.K2low, 44.H1high, 61.C2high) and acne lesional skin (5.C2low, 17.H1low, 42.C1low, 46.C1high, 54.K1high).

Functional screen of *C. acnes* clinical isolates.

For the *C. acnes* strain collection, facial swabs were incubated in RCM, vortexed, and plated onto brucella blood agar plates supplemented with Vitamin K, hemin, and 5% sheep's blood and incubated for 5 days at 37 °C in an AnaeroPak (Thermo Fisher Scientific, Waltham, MA). Resulting small, white colonies that grew were indicative of Cutibacteria species. Roughly 30-50 colonies/per patient were picked using a sterile inoculating loop and transferred to a single well of a deep 96 well plate containing 1 ml of RCM. Following 5 days of anerobic culture, the wells that resulted in visible, turbid growth were selected for screening and transferred to a new deep 96 well plate containing 1 ml of EpiLife supplemented with 50% RCM and 1% glycerol. Plates were cultured for 5 days and strains that grew to at least OD 1.0 (optical density 600 nm) were selected for screening. To functionally screen for inflammatory potential half the culture supernatant was transferred to a 96 well 0.2 μm filter plate and centrifuged at 4,000 x *g* for 15 mins. Sterile glycerol was added to the remaining bacterial culture (at a final concentration of 20%) and the plates were frozen at -80°C for long term storage. Next, 20% sterile culture filtrate was added to SEB-1 cells for 24 h. Supernatant of the SEB-1 cells were then further filtered and transferred to IL-8 ELISA plates (R&D Systems) for quantification.

Single locus sequence typing (SLST)

Putative *C. acnes* colonies cultured on blood agar 5-7 days after anaerobic growth were distinguished from other non-specific colonies like staphylococci, based on size, hemolysis, color, morphology and other morphological properties. Between 15-20 CFU's were picked per patient for SLST. Colonies were picked by sterile toothpick and inoculated into PCR grade water. A volume of this bacterial suspension was used to perform a colony PCR according to (Scholz et al. 2014). Resulting single loci amplicons were subject to PCR purification and submitted for Sanger sequencing. The resulting sequences were submitted to the online *C. acnes* SLST database http://medbac.dk/slst/pacnes to determine the C. acnes sequence type.

Animals and animal care

All animal experiments were approved by the UCSD Institutional Animal Care and Use Committee (protocol no. S09074). SKH-1 hairless mice and WT, $Tlr2^{-/-}$ C57/Bl6 mice were originally purchased from The Jackson Laboratory, bred, and maintained in animal facility of UCSD. Animals in all experimental models were age- and sex-matched.

Mouse model of *C. acnes* skin infection

To promote the formation of acne-like lesions in mice, 100 µl of squalene was topically applied to the backs of age-matched (8 to 10 weeks) SKH-1 mice 24 hours before infection and every 24 hours thereafter throughout the duration of the experiment according to (27).

RNA isolation, cDNA synthesis, and RT-qPCR analysis

Cultured cells and isolated tissues with lysed PureLink Lysis Buffer (Ambion/Life Technologies) and RNA was isolated using the PureLink isolation kit. Up to 1 μg of RNA was reverse transcribed to cDNA using the Verso cDNA synthesis kit (Fisher Scientific). Quantitative real-time PCR were performed the CFX96 Real-Time System (Bio-Rad) using SYBR Green Mix (Biomake, Houston, TX). The housekeeping gene, GAPDH was used to normalize gene expression in samples.

Single cell RNA-Seq analysis.

For scRNA-Seq analysis of mouse skin, the upper back skin of SKH-1 mice were intradermally infected with 1 x 107 CFU of *C. acnes* or RCM control for 3 days. Skin samples were collected from 6 mm punch biopsies and immediately placed on ice. In total, 3 biopsies were pooled per condition (infected or non-infected) for single cell generation. Isolation and analyses of viable single cells were as previously described (O'Neill et al. 2022).

Statistical analysis

Experiments conducted were performed at minimal performed in triplicate with at least three technical replicates. Statistical significance was calculated using a one-way ANOVA with Tukey's multiple comparison test and Student's two-tailed t-test where indicated. *P<0.05, **P<0.01, ***P<0.001, ****P<0.0001 as indicated in figure legends.

Funding:

This work was supported by National Institute of Health grant R01AR074302 (RLG, RM).

Conflict of Interest:

R.L.G. is a co-founder, scientific advisor, consultant and has equity in MatriSys Biosciences and is a consultant, receives income and has equity in Sente Inc.

Acknowledgements:

Data and materials availability:

All data are available in the paper or the supplementary materials. Materials will be made available by contacting RLG and completion of a material transfer agreement. Single cell RNA sequencing data are available for download at gene expression omnibus (GEO) GSE211279 and bulk RNA sequencing data available on the Dryad Server at https://doi.org/10.6076/D1488Z.

Author Contributions:

Conceptualization: AON, RLM, RLG. Methodology: AON, YC, JSS, KJC, FL, THD, LC, SLB, RLM, RLG. Software: JSS, YC, LZ, KJC. Validation: AON, FL, TN, THD, RLM. Formal analysis: AON, JSS, KJC, FL, YC, SB, TN, LZ, THD, LC. Investigation: AON, JSS, KJC, FL, JYC, YLT, THD, LC, TRH, RLM, RLG. Resources: AON, FL, TN, JYC, YLT, TRH, RLG. Data Curation: AON, JSS, KJC. Writing – Original Draft: AON, RLG. Writing – Review & Editing: AON, JSS, KJC, JYC, RLG. Visualization: AON, YC, JSS, KJC, LZ, RLG. Supervision: AON, RLM, RLG. Project administration: AON, RLG. Funding acquisition: RLM, RLG.

REFERENCES

Barnard E, Shi B, Kang D, Craft N, Li H. The balance of metagenomic elements shapes the skin microbiome in acne and health. Sci. Reports 2016 61. Nature Publishing Group; 2016;6(1):1–12 Available from: https://www.nature.com/articles/srep39491

Bordenstein SR, Theis KR. Host Biology in Light of the Microbiome: Ten Principles of Holobionts and Hologenomes. PLoS Biol. PLoS Biol; 2015;13(8) Available from: https://pubmed.ncbi.nlm.nih.gov/26284777/

Caetano AJ, Redhead Y, Karim F, Dhami P, Kannambath S, Nuamah R, et al. Spatially resolved transcriptomics reveals pro-inflammatory fibroblast involved in lymphocyte recruitment through CXCL8 and CXCL10. Zhuan B, Zaidi M, editors. Elife. eLife Sciences Publications, Ltd; 2023;12:e81525 Available from: https://doi.org/10.7554/eLife.81525

Conwill A, Kuan AC, Damerla R, Poret AJ, Baker JS, Tripp AD, et al. Anatomy promotes neutral coexistence of strains in the human skin microbiome. Cell Host Microbe. Cell Press; 2022;30(2):171-182.e7

Davidsson S, Carlsson J, Mölling P, Gashi N, Andrén O, Andersson SO, et al. Prevalence of Flp Pili-encoding plasmids in Cutibacterium acnes isolates obtained from prostatic tissue. Front. Microbiol. Frontiers Media S.A.; 2017;8(NOV):2241

Fitz-Gibbon S, Tomida S, Chiu BH, Nguyen L, Du C, Liu M, et al. Propionibacterium acnes strain populations in the human skin microbiome associated with acne. J. Invest. Dermatol. J Invest Dermatol; 2013;133(9):2152–60 Available from: https://pubmed.ncbi.nlm.nih.gov/23337890/

Hall JB, Cong Z, Imamura-Kawasawa Y, Kidd BA, Dudley JT, Thiboutot DM, et al. Isolation and Identification of the Follicular Microbiome: Implications for Acne Research. J. Invest.

Dermatol. J Invest Dermatol; 2018;138(9):2033–40 Available from: https://pubmed.ncbi.nlm.nih.gov/29548797/

Hay RJ, Johns NE, Williams HC, Bolliger IW, Dellavalle RP, Margolis DJ, et al. The Global Burden of Skin Disease in 2010: An Analysis of the Prevalence and Impact of Skin Conditions. J. Invest. Dermatol. Elsevier; 2014;134(6):1527–34

Holland C, Mak TN, Zimny-Arndt U, Schmid M, Meyer TF, Jungblut PR, et al. Proteomic identification of secreted proteins of Propionibacterium acnes. BMC Microbiol. BMC Microbiol; 2010;10 Available from: https://pubmed.ncbi.nlm.nih.gov/20799957/

Kasimatis G, Fitz-Gibbon S, Tomida S, Wong M, Li H. Analysis of complete genomes of propionibacterium acnes reveals a novel plasmid and increased pseudogenes in an acne associated strain. Biomed Res. Int. 2013;2013

Kelhälä H-L, Palatsi R, Fyhrquist N, Lehtimäki S, Väyrynen JP, Kallioinen M, et al. IL-17/Th17 Pathway Is Activated in Acne Lesions. PLoS One. Public Library of Science; 2014;9(8):e105238 Available from: https://doi.org/10.1371/journal.pone.0105238

Leyden JJ, McGinley KJ, Vowels B. Propionibacterium acnes Colonization in Acne and Nonacne. Dermatology. Karger Publishers; 1998;196(1):55–8 Available from: https://www.karger.com/Article/FullText/17868

McDowell A, Barnard E, Nagy I, Gao A, Tomida S, Li H, et al. An expanded multilocus sequence typing scheme for propionibacterium acnes: investigation of "pathogenic", "commensal" and antibiotic resistant strains. PLoS One. PLoS One; 2012;7(7) Available from: https://pubmed.ncbi.nlm.nih.gov/22859988/

Nagy I, Pivarcsi A, Koreck A, Széll M, Urbán E, Kemény L. Distinct strains of Propionibacterium acnes induce selective human beta-defensin-2 and interleukin-8 expression in

human keratinocytes through toll-like receptors. J. Invest. Dermatol. J Invest Dermatol; 2005;124(5):931–8 Available from: https://pubmed.ncbi.nlm.nih.gov/15854033/

O'Neill AM, Liggins MC, Seidman JS, Do TH, Li F, Cavagnero KJ, et al. Antimicrobial production by perifollicular dermal preadipocytes is essential to the pathophysiology of acne. Sci. Transl. Med. NLM (Medline); 2022;14(632):eabh1478 Available from: https://www.science.org/doi/abs/10.1126/scitranslmed.abh1478

Puhvel SM, Reisner RM, Amirian DA. Quantification Of Bacteria In Isolated Pilosebaceous Follicles In Normal Skin. J. Invest. Dermatol. Elsevier; 1975;65(6):525–31

Ramli R, Malik AS, Hani AFM, Jamil A. Acne analysis, grading and computational assessment methods: an overview. Ski. Res. Technol. John Wiley & Sons, Ltd; 2012;18(1):1–14

Sanford JA, O'Neill AM, Zouboulis CC, Gallo RL. Short-chain fatty acids from cutibacterium acnes activate both a canonical and epigenetic inflammatory response in human sebocytes. J. Immunol. 2019;202(6)

Sanford JA, Zhang LJ, Williams MR, Gangoiti JA, Huang CM, Gallo RL. Inhibition of HDAC8 and HDAC9 by microbial short-chain fatty acids breaks immune tolerance of the epidermis to TLR ligands. Sci. Immunol. American Association for the Advancement of Science; 2016;1(4) Available from: https://www.science.org/doi/abs/10.1126/sciimmunol.aah4609

Scholz CFP, Brüggemann H, Lomholt HB, Tettelin H, Kilian M. Genome stability of Propionibacterium acnes: a comprehensive study of indels and homopolymeric tracts. Sci. Reports 2016 61. Nature Publishing Group; 2016;6(1):1–12 Available from: https://www.nature.com/articles/srep20662

Scholz CFP, Jensen A, Lomholt HB, Brüggemann H, Kilian M. A Novel High-Resolution Single Locus Sequence Typing Scheme for Mixed Populations of Propionibacterium acnes In Vivo.

PLoS One. Public Library of Science; 2014;9(8):e104199 Available from: https://journals.plos.org/plosone/article?id=10.1371/journal.pone.0104199

Vos T, Flaxman AD, Naghavi M, Lozano R, Michaud C, Ezzati M, et al. Years lived with disability (YLDs) for 1160 sequelae of 289 diseases and injuries 1990–2010: a systematic analysis for the Global Burden of Disease Study 2010. Lancet. Elsevier; 2012;380(9859):2163–96

Yu Y, Champer J, Agak GW, Kao S, Modlin RL, Kim J. Different Propionibacterium acnes Phylotypes Induce Distinct Immune Responses and Express Unique Surface and Secreted Proteomes. J. Invest. Dermatol. Elsevier; 2016;136(11):2221–8

Figure 1. Different inflammatory capacity of *C. acnes* strains based on cell type.

(**A-B**) Quantification of secreted pro-inflammatory cytokines by ELISA from from primary human monocyte-derived dendritic cells (hDC) (**A**) and primary human keratinocytes (NHEK) (**B**) at 24 h post-treatment with 15% sterile conditioned media from health-associated *C. acnes* strains (blue) and acne-associated *C. acnes* strains (red). Data shown indicate mean ± SEM. n=3, *p<0.05, **p<0.01, ***p<0.001.

Figure 2. High-throughput typing, and functional screening of *C. acnes* isolates from acne and healthy-derived skin sites. (**A**) Schematic for the high-throughput *C. acnes* screen, including strain collection, isolation, selection, typing and functional readout by ELISA. (**B**) Percentage (%) frequency of the *C. acnes* phylotypes and sequence types identified from swabs of lesional and non-lesional acne skin, including healthy control skin. (**C-E**) IL-8 cytokine release in sebocyte SEB-1 cells 24 h post-treatment with 15% sterile supernatant of *C. acnes* isolates distinguished by source site (C), phylotype IA-1 (D), and SLST (E). (**F,G**) IL8 release in SEB-1 cells 24 h post-treatment with 15% sterile supernatant of all typed *C. acnes* isolates recovered from healthy skin swabs (**F**), and lesional acne skin swabs (**G**). (**H**) Validation and designation of *C. acnes* strains based on inflammatory potential (low, medium (med) and high) and IL-8 release in SEB-1 sebocytes. Optical density (OD600) readings of the *C. acnes* cultures used are indicated on the secondary y-axis. n=3. Data shown indicate mean ± SEM, ns=not significant, *p<0.05, **p<0.01, ***p<0.001, ****p<0.0001 with Ordinary one-way ANOVA with Tukey's multiple comparison test. Each spot represents a single isolate.

Figure 3. *C. acnes* plasmid-positive strains promote greater inflammation *in vitro* and *in vivo*. **(A)** *C. acnes* reference plasmid (NCBI Ref Seq: NC_021086.1) from the strain pIMPLE-HL096PA1 aligned and mapped to *C. acnes* plasmid from strain 46.C1. The 71 coding sequences from both plasmid genomes are illustrated by arrows pointing toward their respective orientation. Protein-coding regions are annotated based on known information from UniProt prokaryotic protein database. Blue lines within alignment indicate percent identity. Sequences are 99.3% identical. The figure was visualized by EasyFig 2.2.2 (**B**) SLST C1- and C2-type *C. acnes* strains were screened for the presence or absence of the linear plasmid based on PCR amplification of the plasmid-borne tight adhesion (tadA) locus. SEB-1 cells were treated for 24 h with 20% sterile supernatant from plasmid-positive (+) and plasmid-negative (-) strains and IL-8 release measured by ELISA. (**C**) List of significantly different Go terms upregulated after treatment with H1 plasmid (+) versus H1 plasmid (-) strains. (**D**) List of significantly different Go terms upregulated after treatment with C1 plasmid (+) versus C1 plasmid (-) strains. (**E**) Heatmap expression of selected genes within the cytokine-mediated signaling GO pathway from NHEKs 4 h post-treatment with 15% RCM (untreated), or 15% sterile supernatant of plasmid-positive (+) and plasmid-negative (-) strains of *C. acnes* H1 or C1 sequence types. (**F**). ELISA of tissue proteins recovered from 8mm biopsies of mouse back skin post-injection of stationary phase *C. acnes* strains. (**G**) CFU counts of the *C. acnes* bacteria recovered from biopsies of mouse back skin 72 h post-injection and normalized to the weight (grams) of the biopsy tissue. n=3-4. Data shown indicate mean ± SEM, *ns*=not significant, *p<0.05, **p<0.01, with two tailed paired Student's t-test.

Figure.4. scRNA-Seq reveals immune activation of distinct cell types associated with the presence of the plasmid. scRNA-seq was conducted on skin lesions 3 days after *C. acnes* infection or mock-infected control skin of SKH-1 mice. **(A)** UMAP plot of all cells passing initial QC, showing cell type assignment based on established lineage markers. **(B)** Bar chart of the number of differentially expressed genes (DEGs) in each major cell type for + plasmid C. acnes versus – plasmid C. acnes. **(C,E,G)** Heatmaps of selected GO terms in fibroblasts (**C**), Keratinocytes (**E**), and Myeloid cells (**G**) enriched during *C. acnes* infection or RCM control mock infection. **(D, F, H)** Violin plots of the expression levels of four selected immune-related genes that had greater enrichment in +P *C. acnes* versus -P *C. acnes* in Fibroblasts (**D**), Keratinocytes (**F**), and Myeloid cells (**H**). n=3 pooled biopsies of 3 mice.

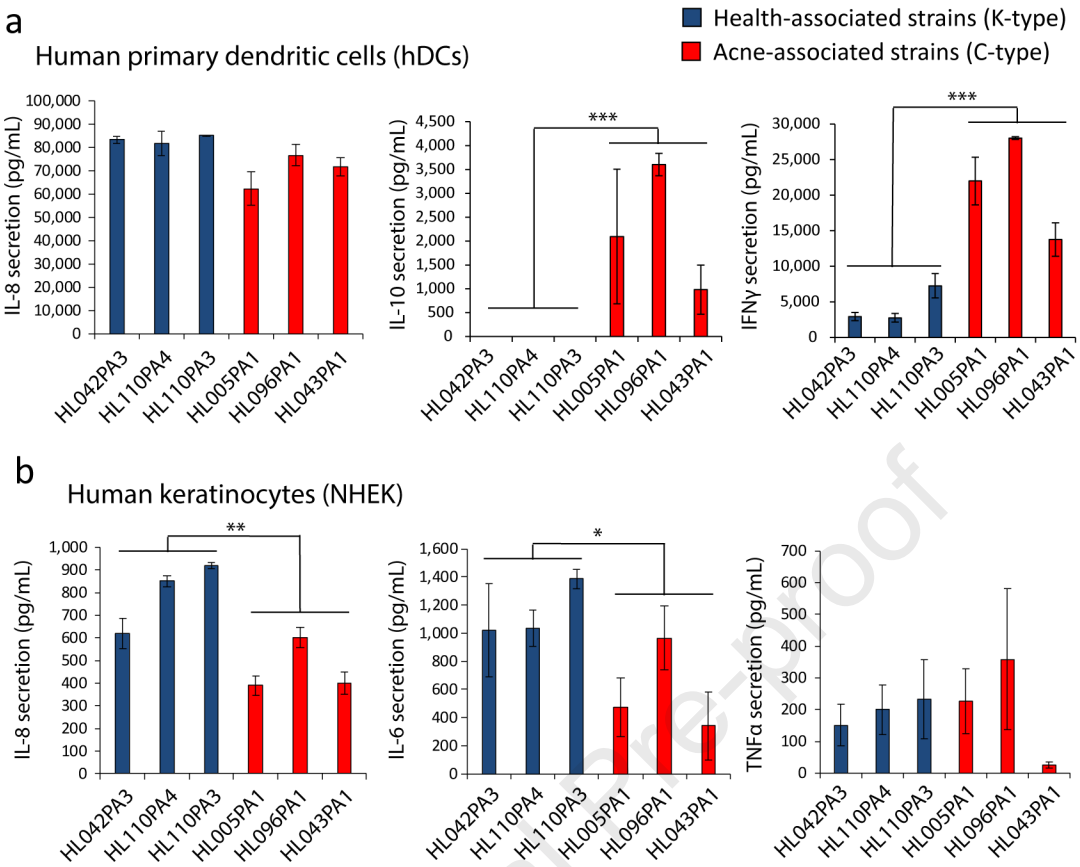

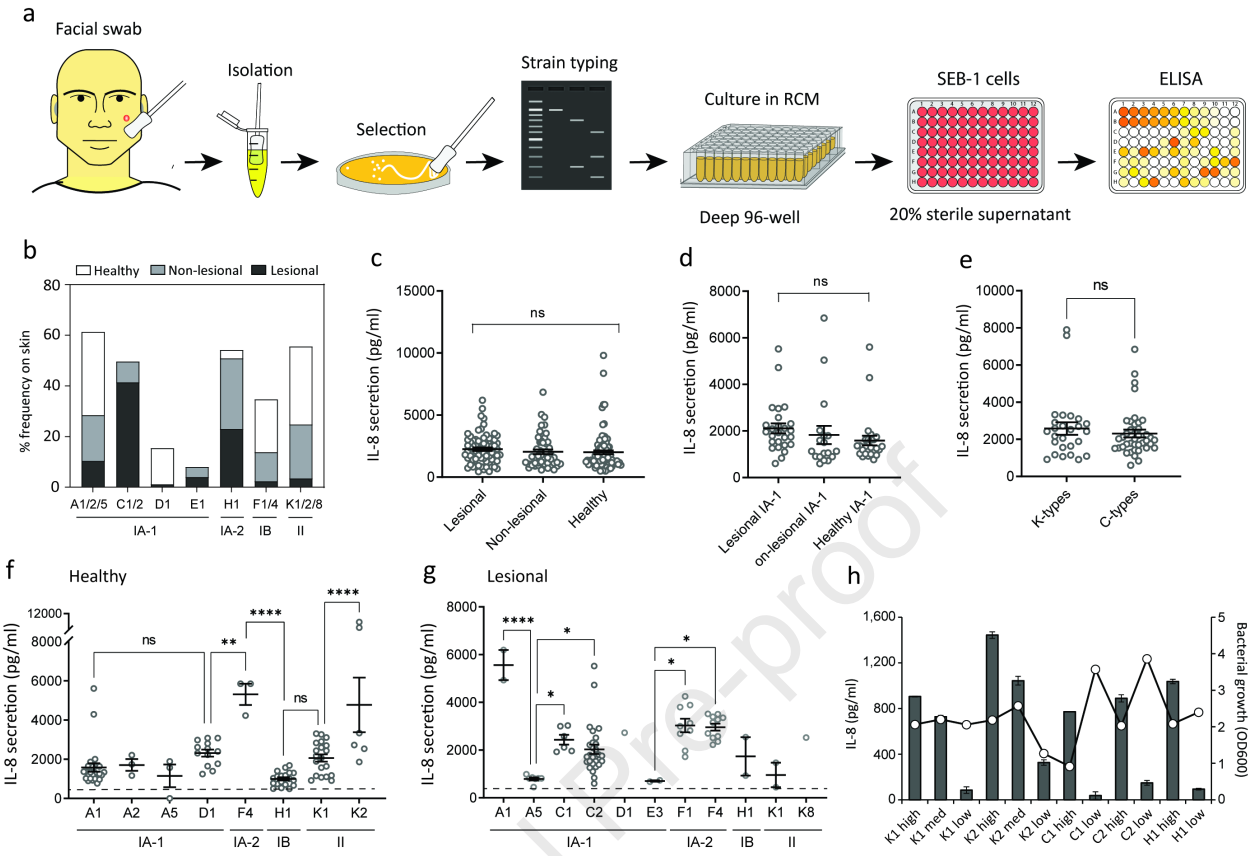

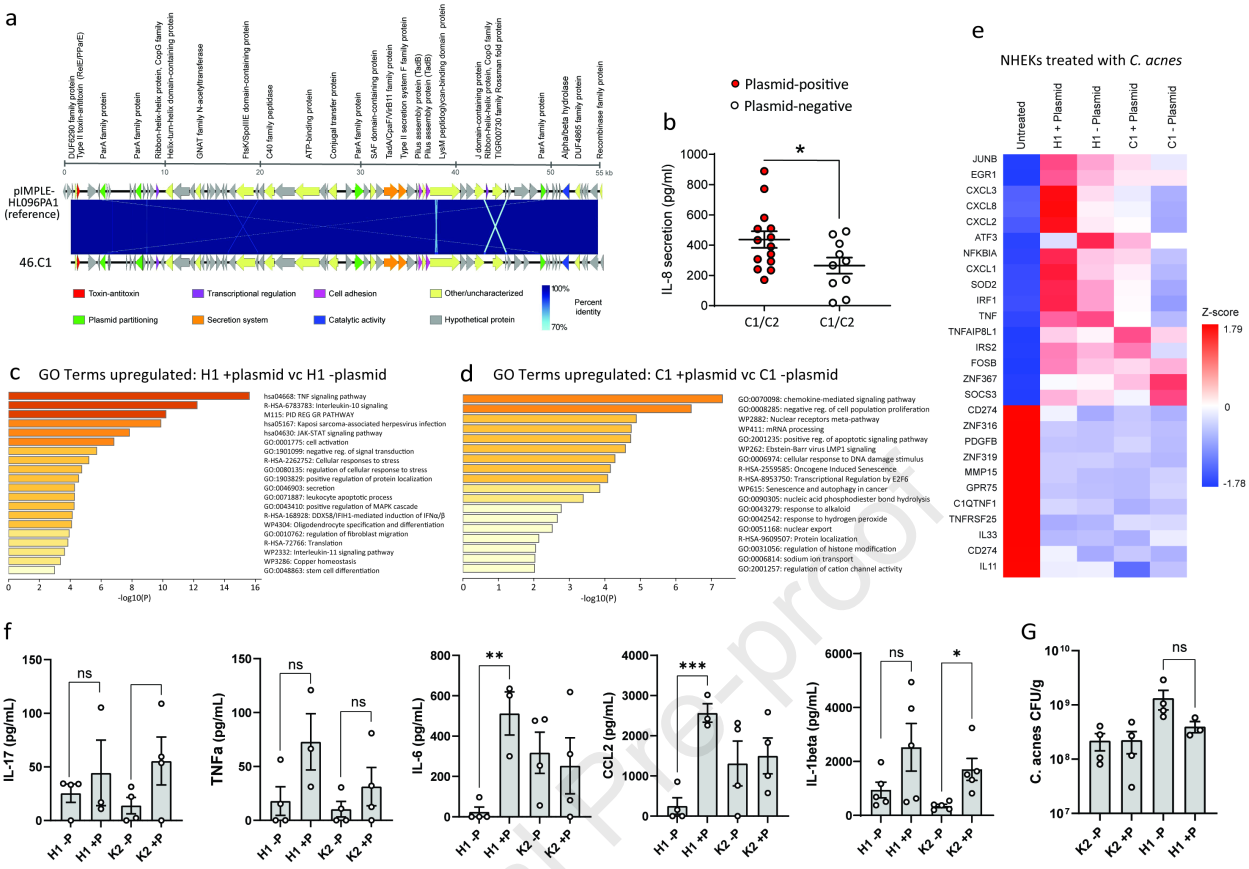

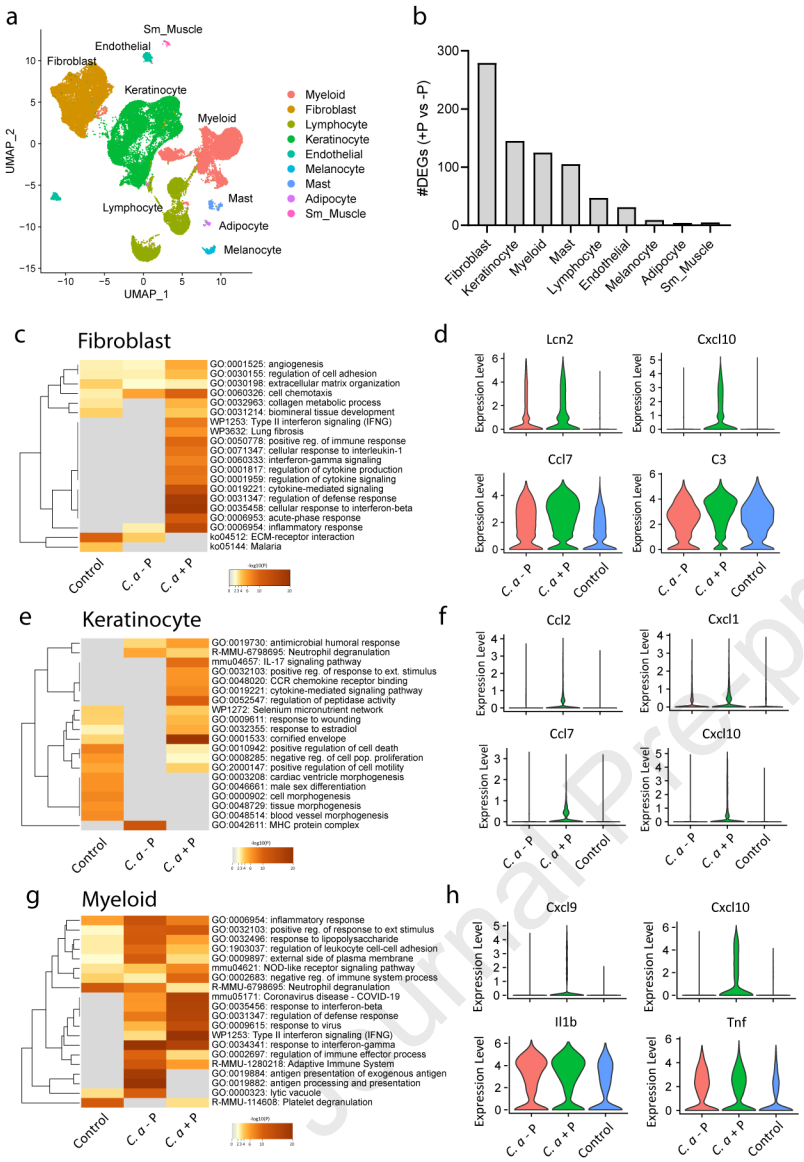

Protein name	NCBI Accession ID	46.C1	61.C1	44.H1	35.K2
Hypothetical protein	N/A				
Hypothetical protein	N/A			1	1
Hypothetical protein	N/A				
DUF6290 family protein	WP_002520161.1	1		1	0.95
Type II toxin-antitoxin system RelE/ParE family toxin	WP_002520160.1	1		1	0.99
Hypothetical protein	N/A	0.94		0.94	
Hypothetical protein	N/A	1		1	
ParA family protein	WP_002520157.1	1		1	
Hypothetical protein	N/A				
Hypothetical protein	N/A	0.67		0.67	
Hypothetical protein	N/A	0.97		0.97	
Hypothetical protein	N/A	1		1	0.92
ParA family protein	WP_032501527.1	0.78		0.78	0.92
Hypothetical protein	N/A	1		1	0.98
Hypothetical protein	N/A	1		1	0.99
Hypothetical protein	N/A	0.99		0.99	0.97
Ribbon-helix-helix protein, CopG family	WP_002520145.1	1		1	0.89
Helix-turn-helix domain-containing protein	WP_015588734.1	1		1	0.96
Hypothetical protein	N/A	1		0.71	0.88
Hypothetical protein	N/A	1		1	0.86
GNAT family N-acetyltransferase	WP_002520142.1	1		1	0.82
Hypothetical protein	N/A	0.93		0.91	0.87
Hypothetical protein	N/A	0.75			0.73
Hypothetical protein	N/A	1			0.76
Hypothetical protein	N/A	0.92	0.9	0.92	0.83
Hypothetical protein	N/A	1	1	1	0.99
Hypothetical protein	N/A	1	1	1	0.99
Hypothetical protein	N/A	1	0.98	1	0.85
FtsK/SpoIIIE domain-containing protein	WP_002520135.1	0.91	0.91	0.91	0.88
Hypothetical protein	N/A	1	1	1	1
Hypothetical protein	N/A	1	1	1	0.99
C40 family peptidase	WP_041446720.1	1	0.95	1	0.95
Hypothetical protein	N/A	1	1	1	0.93
ATP-binding protein	WP_002520130.1	1	1	1	0.99
Hypothetical protein	N/A	1	1	1	0.94
Hypothetical protein	N/A	1	1	1	0.88
Conjugal transfer protein	WP_002520128.1	0.88	0.88	0.88	0.78
Hypothetical protein	N/A	1	1	1	0.91
ParA family protein	WP_002520127.1	0.99	0.99	0.99	0.91
Hypothetical protein	N/A	1	1	1	0.84
SAF domain-containing protein	WP_002520126.1	1	1	1	0.79

Hypothetical protein	N/A	1	1	1	0.88
TadA/CpaF/VirB11 family protein	WP_002522438.1	1	1	1	0.92
Type II secretion system F family protein	WP_002520578.1	1	1	1	0.9
Hypothetical protein	N/A	1	1	1	0.92
Hypothetical protein	N/A	1	1	1	0.84
Pilus assembly protein	WP_002519235.1	0.86	0.86	0.86	0.82
Hypothetical protein	N/A	0.87	0.87	0.87	0.85
Pilus assembly protein	WP_002519237.1	1	1	1	1
LysM peptidoglycan-binding domain-containing protein	WP_015588743.1	1	1	1	0.65
Hypothetical protein	N/A	1	1	1	0.68
Hypothetical protein	N/A	1	1	1	0.96
J domain-containing protein	WP_002520572.1	1	1	1	0.63
Ribbon-helix-helix protein, CopG family	WP_015588744.1		0.91		0.84
TIGR00730 family Rossman fold protein	WP_002522196.1	0.97	0.98	0.97	0.97
Hypothetical protein	N/A	0.88	0.88	0.88	0.88
Hypothetical protein	N/A	0.84	0.84	0.84	0.81
Hypothetical protein	N/A			1	
Hypothetical protein	N/A	1	1	1	
ParA family protein	WP_032501527.1	0.98	0.98	0.98	
Hypothetical protein	N/A	1	1	1	
Hypothetical protein	N/A	1	1	1	
Hypothetical protein	N/A	0.99	0.99	0.99	
Hypothetical protein	N/A	1		1	
Alpha/beta hydrolase	WP_002518866.1	1	1	1	
DUF4865 family protein	WP_002518867.1	1	1	1	
Hypothetical protein	N/A				
Hypothetical protein	N/A	1	1	1	
Hypothetical protein	N/A	1	1	1	
Hypothetical protein	N/A	0.86	0.86	0.97	
Recombinase family protein	WP_073859749.1			0.95	

Supplementary Figure 1. Amino acid sequence comparison of the *C. acnes* reference plasmid pIMPLE-HL096PA1 to assembled plasmids from strains 46.C1, 61.C2, 44.H1, and 35.K2. 71 coding sequences within *C. acnes* reference plasmid (NCBI Ref Seq: NC_021086.1) from the strain pIMPLE-HL096PA1 were aligned to the coding sequences within four plasmids from *C. acnes* strains 46.C1 and 61.C2, 44.H1, and 35.K2. Percent sequence identity was calculated using the Levenshtein distance algorithm. Sequences from reference plasmid with 60% identity or higher were reported. The 25 non-hypothetical proteins are indicated in yellow. Proteins from the reference sequence sharing 90% identity or greater to plasmids sequenced in this paper are indicated in green.

SUPPLEMENTARY MATERIALS AND METHODS

Cell Culture

Normal neonatal human primary epidermal keratinocytes (NHEKs) were cultured in Epilife complete medium containing 60 mM CaCl2 supplemented with 1X human keratinocyte growth supplement and a 1X antibiotic-antimycotic at 37°C and 5% CO2. NHEKs were used only for experiments between passages 3 to 5. NHEKs were grown to approximately 80% confluency prior to experimentation. Human monocyte-derived dendritic cells (hDC) were isolated from human peripheral blood mononuclear cells (PBMC) prepared by centrifugation on a Ficoll gradient. Blood CD14+ monocytes were isolated from PBMC by positive selection using anti-CD14-coated magnetic beads according to manufacturer's instructions (Miltenyi Biotek). The adherent monocytes were cultured in DMEM supplemented with 10% FBS supplemented with 600 U/mL GM-CSF and 20ng/mL IL-4. On day 4, the medium was replenished containing GM-CSF, IL-4, and TNF-a (final concentration, 10 ng/mL). After 7 days of culture, the cells were washed and replaced with DMEM/FCS. hDCs were serum starved for 4 h prior to experimentation and for the duration of the treatment. For bacterial supernatant treatments, differentiated NHEKs and hDCs were treated with sterile-filtered bacterial supernatant at 15-20% (vol) in Epilife medium for 4 h or 16-24 h (as indicated). Sebocyte SEB-1 cells were cultured in were maintained in Sebomed Basal Medium supplemented with 10% FBS, and recombinant human epidermal growth factor (rhEGF, 5 ng/mL) at 37°C in 5% CO2. Cells were passaged before reaching 100% confluency in tissue culture flasks. For experiments, cells were switched to medium containing 1% FBS overnight before stimulation. For RNA extraction, the cells were washed 2X in PBS and lysed with PureLink lysing Buffer supplemented with β-mercaptoethanol. RNA was purified according to manufacturer's instructions. For protein

Reagents and chemicals

rIL-4 (10 μg), rTNFα (10 μg), rIFNγ (10 μg) and LPS was purchased from Biolegend. Anaerogen sachets (OXAN0025A) was purchased from Fisher Scientific. GasPak EZ (B260683) was purchased from Fisher Scientific. MALP-2 was purchased from Enzo Life Sciences. Synthetic LL-37 was purchased from Genemed synthesis. Lauric acid (W261416) was purchased from Sigma Aldrich. Synthetic CRAMP peptide was purchased from Sigma-Genosys. IL-8 ELISA (BDB555244) and IL-6 ELISA (BDB555220) were purchased from Fisher Scientific. IL-17, IL-10, CCL2, and TNFα ELISA Duoset were purchased from Fisher Scientific. Complete protease inhibitor cocktail tablets (11697498001) were purchased from Fisher Scientific.

Mouse model of *C. acnes* skin infection

To promote the formation of acne-like lesions in mice, 100 μl of squalene was topically applied to the backs of age-matched (8 to 10 weeks) SKH-1 mice 24 hours before infection and every 24 hours thereafter throughout the duration of the experiment according to (27). Mice were intradermally injected with approximately 1 × 107 CFU of *C. acnes* or control (RCM). Images of mouse back skin were taken with a Panasonic Lumix TS30 digital camera. At 3-day post-injection, mice were sacrificed, and an 8-mm skin biopsy of the infected region was retrieved. For protein extraction, skin samples were cut into small pieces using a sterile scalpel then digested in RIPA buffer supplemented with protease inhibitors for 60 min on ice, vortexing intermittently every 5 min. Tubes were centrifuged at 10,000x *g* for 10 mins at 4°C and the supernatant harvested. Protein concentration was quantified by Pierce BCA assay kit and normalized to 500 μg/ml. Selected cytokines were quantified by ELISA according to manufacturer's instructions.

Single cell RNA-Seq analysis

The 10X Genomics Cell Ranger version 3.0.1 software pipeline with default parameters was used to perform sample demultiplexing, barcode processing, alignment to the mm10 reference genome, and single-cell gene counting. Data were further filtered, processed and analyzed using the Seurat R toolkit version 3 (22,23). Filtering of initial data involved selecting cells with > 100 features and < 10% mitochondrial genes. Data were normalized and scaled and variable genes identified using the function scTransform(). Principal components (PCs) were calculated from these variable genes using RunPCA() and the top 30 PCs were used for downstream analysis. Clusters were identified using FindNeighbors() then FindClusters()with argument resolution = 2.0. Nonlinear dimensionality reduction and visualization was performed with UMAP using the RunUMAP() function. Marker genes for each cluster were determined using FindAllMarkers() with parameters only.pos = TRUE, min.pct = 0.25, and thresh.use = 0.25. Clusters were assigned to cell types “Myeloid”, “Fibroblast”, “Lymphocyte”, “Keratinocyte”, “Endothelial”, “Melanocyte”, “Mast”, “Adipocyte”, and “Sm Muscle” based on marker genes. 14 out of the original 53 clusters were annotated as fibroblasts and underwent additional quality control. In brief, a new Seurat object was generated using only the cells in these clusters with their corresponding raw counts, followed by normalization, scaling, clustering and dimensionality reduction as described above, resulting in 15 fibroblast clusters with FindClusters() resolution argument = 0.6. Clusters with high expression of leukocyte, keratinocyte, and adipocyte marker genes as well as cell cycle genes were excluded. A final Seurat object was created from the remaining cells and their raw counts with a final iteration of normalization, scaling, clustering and dimensionality reduction resulting in 12 fibroblast clusters with FindClusters() resolution

argument = 0.6. Marker genes were identified on the three groups with FindAllMarkers() with parameter only.pos = TRUE and thresh.use = 0.25. Gene ontology analysis was performed on marker genes using Metascape (24).

Whole genome sequencing and plasmid assembly

Overnight cultures of 12 *C. acnes* strains were pelleted by centrifugation at 10,000 x g for 5 mins and transferred to a -80°C freezer. The bacterial pellets were shipped to The Sequencing Center (Fort Collins, CO) for genomic DNA extraction, library preparation, and Illumina short-read sequencing. First, sequencing adapters were trimmed using Trimmomatic v0.39 (25). Overlapped reads were merged using FLASH v.1.2.11 (26) to support the generation of longer reads from fragment libraries before genome assembly. Thirdly, reads were assembled using Spades v.3.12.0 with the following parameters: --*merge* to indicate merged forward and reverse paired-end reads and --*plasmid* to initiate the plasmidSPAdes algorithm for plasmid-specific detection and assembly (27). A fully assembled plasmid mapped onto one contig was achieved for *C. acnes* strain 46.C1. This plasmid sequence was annotated using Prokka v.1.12 with default parameters to obtain the location and translation of each coding sequence (CDS) and the putative proteins were identified through the Uniprot prokaryotic database. Next, the C. acnes reference plasmid was mapped to *C. acnes* plasmid from strain 46.C1 using EasyFig 2.2.2 default parameters to show percent identity across the genome and the 71 coding sequences (Figure 3A). Gray arrow annotations indicate hypothetical proteins. The 25 non-hypothetical proteins' recognized names from the NCBI reference are reported respectively above their genome annotation. Other colored arrows indicate whether the non-hypothetical protein is present in the 46.C1 plasmid and any known information on protein functionality according to UniProt.

Plasmid sequences from all C. acnes strains (46.C1, 61.C1, 44.H1, and 35.K2) were each independently compared to the C. acnes reference plasmid pIMPLE-HL096PA1 (NCBI Ref Seq: NC_021086.1). First, all plasmid sequences of interest were annotated using Prokka v.1.12, as mentioned previously. Next, using an in-house Python script, Biopython-SeqIO v.1.79 was used to parse the GenBank files for CDS features from each annotated plasmid of interest. For each of the four plasmids in this study, the 71 CDS regions from pIMPLE-HL096PA1 were independently aligned to every CDS region to identify the analogous or highest similarity region (Suppl. Fig 1). Percent identities were calculated from Levenshtein (edit) distance using Python-Levenshtein v.0.12.2. The highest percent match, if greater than or equal to 60%, was reported, with a value of 1 indicating a 100% sequence match of a CDS region between reference and the plasmid of interest.

Supplementary Figure 1. Amino acid sequence comparison of the *C. acnes* reference plasmid pIMPLE-HL096PA1 to assembled plasmids from strains 46.C1, 61.C2, 44.H1, and 35.K2. 71 coding sequences within *C. acnes* reference plasmid (NCBI Ref Seq: NC_021086.1) from the strain pIMPLE-HL096PA1 were aligned to the coding sequences within four plasmids from *C. acnes* strains 46.C1 and 61.C2, 44.H1, and 35.K2. Percent sequence identity was calculated using the Levenshtein distance algorithm. Sequences from reference plasmid with 60% identity or higher were reported. The 25 non-hypothetical proteins are indicated in yellow. Proteins from the reference sequence sharing 90% identity or greater to plasmids sequenced in this paper are indicated in green.